JMEPEG (2012) 21:1962–1969
DOI: 10.1007/s11665-011-0102-2

1059-9495/$19.00

Characterization of Failed Surface of Ti and Imidex (PI) Film for Different Inter-layer Thicknesses of Ti Film

Nusrat Lubna, Zariff Chaudhury, and Golam Newaz

(Submitted January 10, 2011; in revised form December 6, 2011)

For miniaturized biomedical devices, laser joining of dissimilar materials offers excellent potential to make precise joints. An important system for consideration is titanium (Ti) coated glass joined with biocompatible imidex polyimide (PI). Metallic Ti with various thicknesses was deposited on top of pyrex 7740 borosilicate glass by using DC-magnetron sputtering deposition method. Effect of bond strength between Ti coated glass and imidex polyimide (PI), due to thickness variation of sputtered Ti coating was studied. Three different Ti inter-layer thicknesses were considered, 50, 200, and 400 nm. Tests results indicated that the thinner film produced lower shear strength and higher thickness produced higher shear strength. It has been observed that thicker film (200 and 400 nm) enhanced considerably the bond strength with enhancing the film roughness as well. Higher roughness resulted in more contact area at the interface, results higher number of chemical bonds and increased mechanical interlocking; which in turn increase the laser joint strength. For stronger bond with higher thickness, mixed mode failure was observed which included cohesive failure of polymer, interface failure of Ti/glass and failure on the glass itself. On the other hand, for weak bond with thinner film, mostly interface failure was observed for this system of Ti coated glass/imidex. For thicker film, chemical bond of Ti-C and Ti-O were observed. The role of both surface characteristics and chemical bonding for laser joints were investigated by using advanced techniques such as X-ray photoelectron spectroscopy, scanning electron microscopy, and energy dispersive spectroscopy.

Keywords bond strength, inter-layer thicknesses, mechanical interlocking, roughness, SEM, XPS

1. Introduction

Thermoplastic polymers, such as polyimide have diverse applications, such as gas separation membranes and as insulating layers in microelectronic device fabrication due to their superior mechanical and dielectric properties, excellent thermal stability, and chemical resistance (Ref 1), as a fabrication material for intracortical neural implant (Ref 2), thin film packaging in probe circuitry (Ref 3), and also in micro- and nano-fluidic channels due to its favorable electric and mechanical properties and its biocompatibility (Ref 4). Biocompatible materials such as titanium and polyimide are potential candidates in encapsulating implant devices. In anticipation of use with bio-implants, previous researchers in our group studied the effect of artificial cerebrospinal fluid (physiological saline with a low concentration of other salts) on the joint strength for titanium foil/imidex polyimide system (Ref 5). Ti/polyimide interfaces obtained by laser joining were also studied by our research group with X-ray photoelectron spectroscopy (XPS) in order to clarity the chemistry of the joint formation (Ref 6).

There are different technologies of joining two dissimilar materials, e.g., ultrasonic bonding and conventional heating. However, these techniques are bulk joining techniques. Compared to these joining techniques the transmission laser joining exploits *localized* laser heating effect and low temperature bonding materials for sealing and encapsulation of temperature sensitive devices. It includes short bonding time (seconds as compared to tens of minutes in the conventional bonding process), low thermal damage, and low cost. Because of localized heating the temperature rise experienced by a MEMS device can be substantially lower than the actual bonding temperature. This effect is extremely desirable for assembly and packaging of MEMS devices with low temperature tolerance. Another advantage over ultrasonic bonding is that the entire device is subjected to high frequency vibration which can have unwanted effects in the device.

Although bonding of dissimilar material has been studied, the combination of polyimide and Ti is not well studied, particularly, in the context of micromechanisms of bonding and interfacial characterization for laser transmission bonding. We focused our attention to understand how good quality bonds are formed in these materials with clear understanding of material attributes and physical dimension such as thickness. In this article, the thickness effect of sputtered titanium thin film on the bond strength of Ti coated glass and imidex polyimide was studied. Imidex film used in this study was made from Aurum resin. This thermoplastic and semi-crystalline polyimide have a glass transition temperature of 250 °C and melting temperature of 388 °C (Ref 7, 8). A key question is whether the Ti film thickness needs to meet certain thickness to form good bonding with polymer. This article considers this question and based on

Nusrat Lubna, Department of Material Science and Chemical Engineering, Wayne State University, Detroit, MI; **Zariff Chaudhury**, Metallurgical Technology Program, College of Agriculture & Technology, Arkansas State University, Jonesboro, AR; and **Golam Newaz**, Department of Mechanical Engineering, Wayne State University, Detroit, MI. Contact e-mails: lubna@wayne.edu and nusrat.lubna09@gmail.com.

that samples were prepared for different thicknesses of Ti. Samples of titanium coated glass with imidex for three different thicknesses of Ti film (50, 200, and 400 nm) were analyzed by means of mechanical lap shear test to get bond strength measurement. For failure mode assessment, scanning electron microscopy (SEM) and XPS were done. SEM provided a clear view for surface morphology and XPS helped to understand the chemical bond information on the surface. Novelty of our research is that a set of characterization procedures are combined to assess the quality of the bond at microscale characterization whereas a single technique may not have been adequate. Results from our research will help in developing strong bonds using laser transmission technique and it also advances the knowledge in the field.

2. Experimental

2.1 Sample Preparation

For the purpose of this work thin films of titanium were deposited in the vacuum chamber by using a DC-magnetron sputtering system. Before deposition, glass substrates (10×20 mm^2 and a thickness of 0.5 mm) were cleaned in ultrasonic bath for 15 min each step inside a fume hood: (i) in a degreasing soap solution (alconox), (ii) rinsed with DI water then blow with nitrogen, (iii) cleaned by acetone then blow it with nitrogen, and (iv) and at last cleaned with methanol then blow it with nitrogen.

These Ti coated glass samples were laser-joined to 0.18 mm thick polyimide imidex (Wastelake Plastic Company) by using radiation from a 25 W cw Yb-doped fiber laser operating at $\lambda = 1100$ nm. The laser beam has Gaussian power profile and a beam diameter of 0.2 mm. Clamping pressure of 60 psi was applied for the Ti coated glass/polyimide sample. A scanning speed of 100 mm/min, defocus of 1.9 mm, laser power of 0.87, 0.89, and 0.93 W were used for 50, 200, and 400 nm thick titanium sputtered film, respectively, to produce the joint line. Figure 1(i) shows the schematic diagram of the transmission laser joining process.

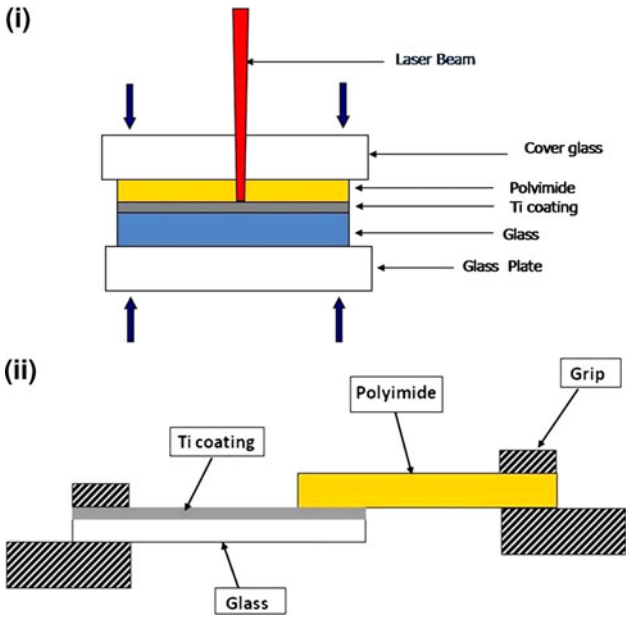

Fig. 1 (i) Laser transmission joining of two materials using a laser beam. (ii) Schematic of a Ti coated glass/PI system

Since the optical properties of the materials play a decisive role for this joining technology, an optimization of absorbers and material conditions is of crucial importance for high quality joints. The applicability of laser joining for a specific material combination and the selection of the appropriate approach depends on the optical properties of the materials. Based on the optical properties, the appropriate laser wavelength was selected to pursue the bonding. A preferred approach for materials with different optical properties is transmission joining (Ref 9, 10) in an overlap configuration. In this case, both materials were clamped on top of each other and the joint was created directly at the interface between the two parts based on the localized heat input of the laser. This was achieved by selecting a laser wavelength that can penetrate the top material and then absorbed at the surface of the bottom material. Transmission joining has a potential application for joining dissimilar material like polyimide-to-metal (Ref 10, 11). This process is used for joining plastics, silicon or glass using total or partial transmission of the different materials and performing hidden joints inside a component (Ref 12).

2.2 Apparatus

The bond strength measurement for the samples were carried out by using a 6-axis sub-micron tester (Ref 13), which is a general-purpose micromechanical/thermal testing instrument, fully controlled by a PC computer. It allows the application of displacements/loads to the tested specimen along six degrees of freedom, i.e., three orthogonal translations and three rotations. The displacement resolution of each closed-loop, DC-motor-drive stage was maintained at 0.1 mm in translations and 0.001° in rotations. A capacitance gage or a linear encoder was used to measure the actual displacement of a test sample. Schematic diagram of the Ti coated glass/polymer system prepared for lap shear test is shown in Fig. 1(ii). The failure loads obtained for all samples were normalized by the joint area as measured by the optical microscopy.

The SEM along with EDS investigations were carried out with Philips XL 30 SEM-FEG/EDS instrument using a beam energy of 30 keV. The energy dispersive spectroscopy (EDS) used was made by EDAX, INC. Both the PI side and titanium coated glass surface sides were studied. To avoid charging effects, the PI side part was sputter-coated with a thin gold (Au) layer prior to the SEM imaging.

The XPS analysis were carried out with a Perkin Elmer, model 5500 XPS spectrometer under high vacuum conditions (7×10^{-10} torr), Al Kα X radiation with an energy of 1486.6 eV was utilized. The binding energies (BE) were referenced to the C 1s line at 284.6 eV.

3. Results and Discussion

3.1 Bond Strength Evaluation

To evaluate the bond strength for all the samples, mechanical lap-shear test were performed. In a lap-shear test, samples were mounted in a micro-tester. By monitoring all 6-axis forces and moments, and releasing any unnecessary mounting forces by micropositioning the corresponding stages during or after

mounting the sample, those undesirable forces/moments were reduced to zero. The failure loads obtained for all samples were divided by the joint area (bond length × bond width). The bond length and bond width were measured by using an optical microscope (Olympus model BX 60). Imidex and 50 nm Ti coated glass produced laser joint with shear strength of 22 ± 4.7 MPa ($n = 18$); whereas, Imidex and 200 nm Ti coated glass produced laser joint with shear strength of 29 ± 3.4 MPa ($n = 22$) and 400 nm Ti coated glass produced laser joint strength of 29 ± 6.6 MPa ($n = 21$). In these three cases the laser parameters were same except laser power. During laser micro-joining process we have used 0.93, 0.89, and 0.87 W, respectively, for 400, 200, and 50 nm coatings on glass surfaces. The roughness of this thin 50 nm film is only 3 nm, which is more than three times smaller than the roughness of 200 nm (10.5 nm) and almost six times smaller than the roughness of 400 nm thick film. Higher roughness resulted in more contact area at the interface, a higher number of chemical bonds and increased mechanical interlocking, which in turn increase the laser joint strength. For 50 nm low surface roughness and lack of mechanical interlocking property causes weak bonding between metal and polymer. It seems the main factor influencing the failure is film thickness which ultimately related with film roughness. Rougher film is likely to provide better mechanical interlocking. At the same time rougher film provides better thermal dissipation of local heat, which is essential for good bonding (Ref 14). Thin Ti film properties and laser joint strength of these three thicknesses are presented in Table 1.

3.2 SEM Analysis

To investigate more about the locus of failure, the SEM analysis along with EDS were done for these different adhesion layer thicknesses. From SEM/EDS analysis (Fig. 2) for thinner film (50 nm) transfer of very tiny amount of glasses are observed. Also transfer of titanium onto PI surface is very insignificant. No transfer of PI is observed. These pictures clearly represent interface failure. For 200 nm thick Ti coated glass/PI system, SEM/EDS analysis (Fig. 3i) shows that some titanium has removed from the titanium surface and good amount of glass and titanium are on the surface of polyimide (Fig. 3ii). It is observed from the SEM images along with EDS spectrum for the titanium surface, that a good amount of imidex is transferred to the titanium surface (Fig. 3i). Crack initiation and propagation of the film is also noticed. The SEM image of imidex side of the lap shear tested sample evidencing deformation of polymer due to cohesive failure of polymer. Broken pieces of glass and titanium confirm that they are transferred from the titanium surface. Based on investigation of SEM/EDS analysis, it can be reported that cohesive failure of polymer is taking place and titanium surface confirms the presence of polymer on the titanium surface. Locations where glass failure took place presence of titanium were hard to detect. Because the thickness of glass is 0.5 mm which is tremendously higher compared to a film thickness of only 200 nm. That is why locations where only glass failure occurred titanium is hard to detect as it is underneath the pieces of glass. EDS picture of polyimide (PI) side of the surface confirms that good amount of titanium and glass are transferred to that surface. So it can be concluded that for 200 nm thick film mixed mode of failure is taking place; cohesive failure which occurred inside of the polyimide near the titanium/imidex interface, failure on titanium/glass interface and failure on the glass itself.

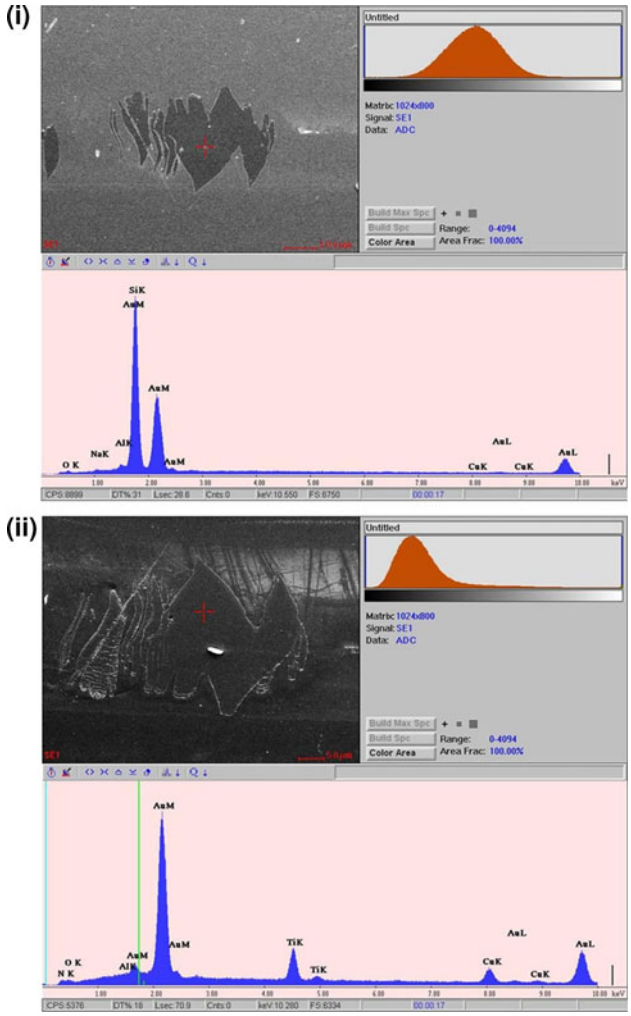

Fig. 2 SEM/EDS analysis of 50 nm thick Ti coated glass/PI system: (i) failed Ti surface, (ii) failed PI surface

Table 1 Surface roughness of different thicknesses of Ti film prepared on Pyrex 7740 glass substrate and laser joint strength data

Sample type	Coating roughness, nm	No. of sample	Joint strength, MPa
50 nm Ti coated glass/imidex (PI)	3	18	22 ± 4.7
200 nm Ti coated glass/imidex (PI)	10.5	22	29 ± 3.4
400 nm Ti coated glass/imidex (PI)	17	21	29 ± 6.6

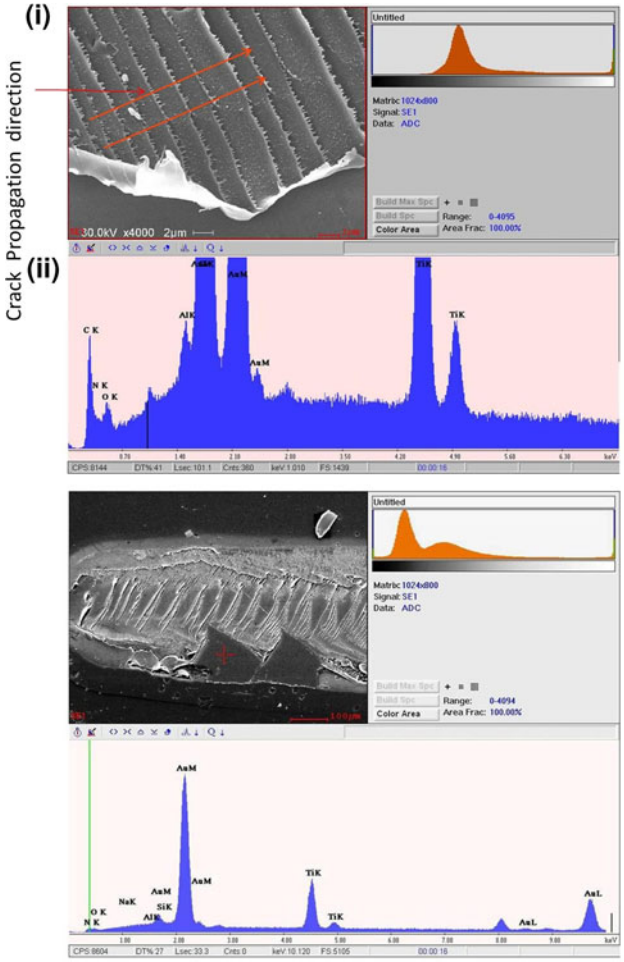

Fig. 3 SEM/EDS analysis of 200 nm thick Ti coated glass/PI system: (i) failed Ti surface, (ii) failed PI surface

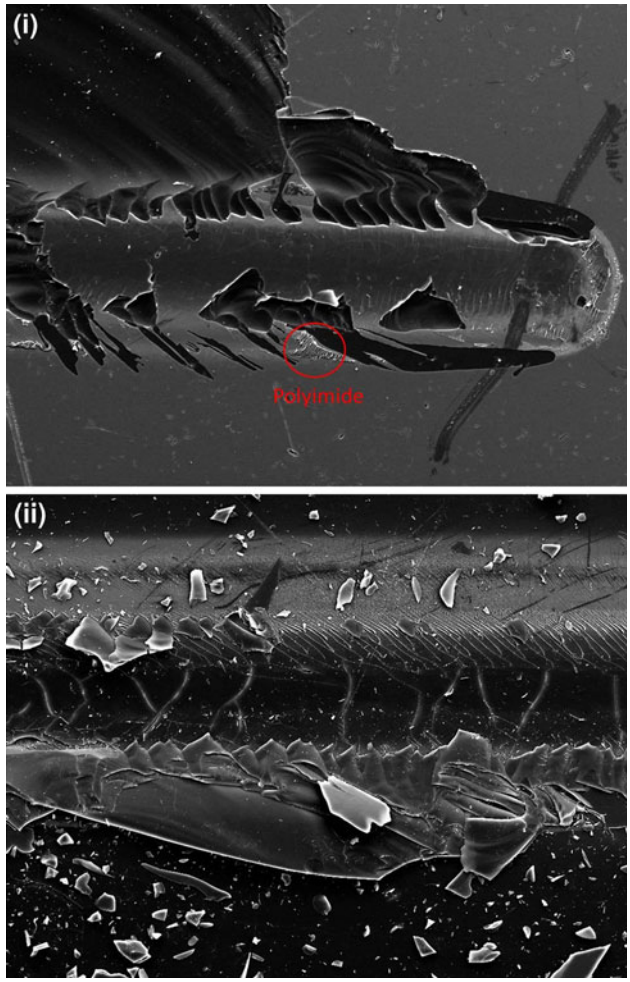

Fig. 4 SEM analysis of 400 nm thick Ti coated glass/PI system: (i) failed Ti surface, (ii) failed PI surface

SEM analyses are also conducted for the samples with titanium coating thickness of 400 nm. A huge amount of glass pieces are observed on the polyimide surface. SEM analysis (Fig. 4) shows presence of glass on both surface; this means that titanium is transferring with good amount of glass on polyimide surface indicated glass failure and titanium/glass interface failure. SEM picture of titanium surface clearly shows presence of imidex; indicated cohesive failure of polymer. For the samples with thicker films (200 and 400 nm) a very strong bond strength were obtained, also failure modes are mixed mode: cohesive failure of polymer, titanium/glass interface failure, and glass failure. It can be interpreted that because of the good bonding, instead off PI/titanium interface failure, failure occurred in the glass and also partially occurred onto the glass/titanium interface. Cohesive failure of polymer for these 200 and 400 nm thick films is a strong indication of good bonding.

For metal film, conductivity is expected to decrease as film thickness is reduced (Ref 15). So, thicker titanium metal film has the higher conductivity. Low conductivity of thinner film (50 nm) results elevation of temperature compared to other two systems (200 and 400 nm). This might results degradation of PI in the case of thinner film. The outcome is more voids on the PI side and results in cohesive strength decreases. So, debonding took place on interface for 50 nm and failure occurred on the interface.

Figure 5(a)-(c), showed the plane view of SEM micrographs of sputtered Ti thin film of 50, 200, and 400 nm thicknesses. The SEM micrograph of 50 nm thin film exhibits crack-like structure (Fig. 5a). The cracks are voided boundaries and create small islands all over the surface. Two types of growth is observed for this 50 nm thin film—(i) island growth and (ii) lateral growth. For 200 and 400 nm thick film (Fig. 5b, c), Ti film appears to be continuous with no voided-boundaries. It seems that critical thickness of film to get a continuous film with no voids must be over 50 nm. Not having enough volume might be another reason for not forming good bond for thinner film during laser joining process.

3.3 XPS Analysis

The XPS survey spectrum for the failed Ti surface (thickness of 50 nm) and corresponding imidex surface were done on interface of the laser joint (Fig. 6i-ii). Figure 6(i) is the XPS survey spectra for failed Ti surface. The survey spectra of XPS showed significant peaks for O 1s, C 1s, and Ti 2p3 on failed Ti surface. No evidence of N was observed. This indicates that no imidex was transferred to the Ti surface. Spectra in Fig. 6(ii) showed significant peaks for C 1s, O 1s, and N 1s. No evidence of Ti 2p3 was observed. This indicates no transfer of Ti to the polymer surface. The failure locus is clearly on the interface. In case of 200 nm Ti coated glass/PI

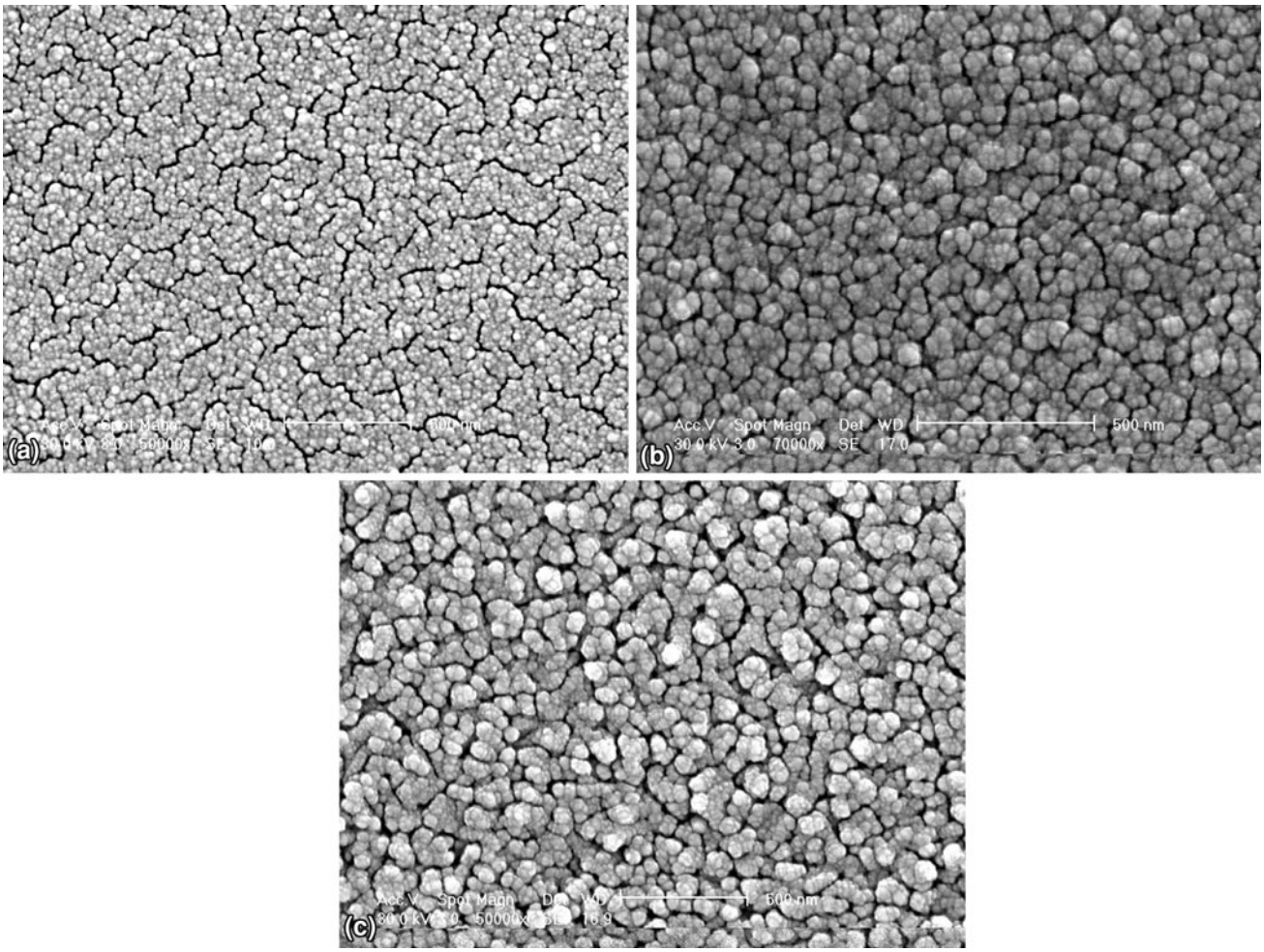

Fig. 5 (a) SEM micrograph for sputtered Ti film on glass (50 nm thick Ti coating); (b) SEM micrograph for sputtered Ti film on glass (200 nm thick Ti coating); (c) SEM micrograph for sputtered Ti film on glass (400 nm thick Ti coating)

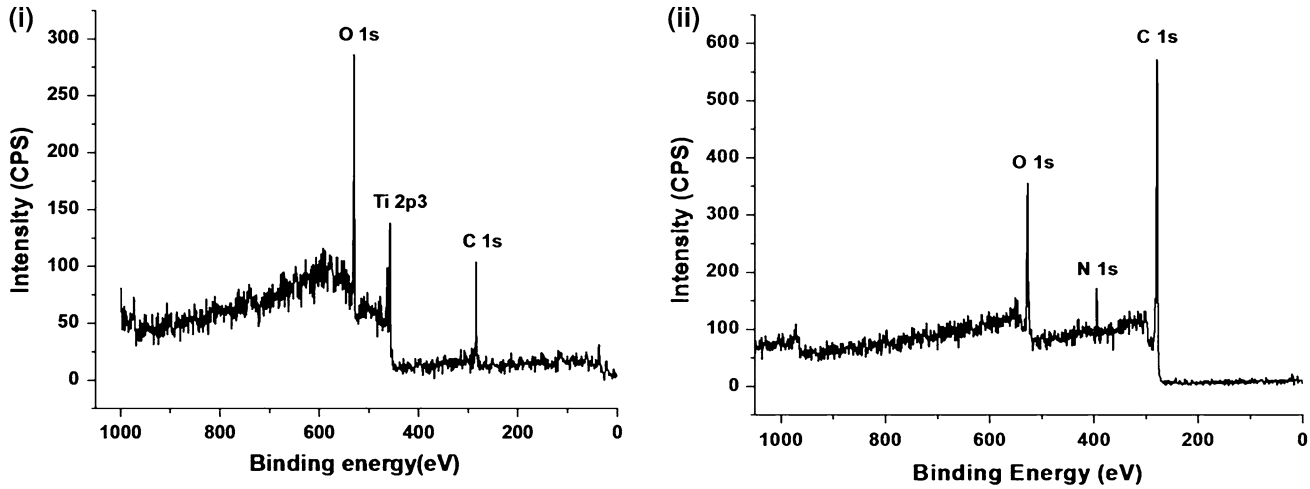

Fig. 6 XPS survey spectra taken on-joint for 50 nm thick Ti coated glass/PI system: (i) failed Ti side, (ii) failed PI side

system high resolution spectra (Fig. 7a) showed that the C 1s spectrum taken from the on-joint area of the Ti surface (sputtering = 0 s) consists of a intense peak at 284.5 eV with a shoulder at around 286 eV and a small peak at 288-289 eV, can be attributed to C from the polymer chain. The intense peak at 284.5 eV is from the mixture of C-C, C-H, and C-O bonds (Ref 16, 17). After sputtering the intensity of the C peak is decreasing, while a new peak at around 282.3 eV is emerging.

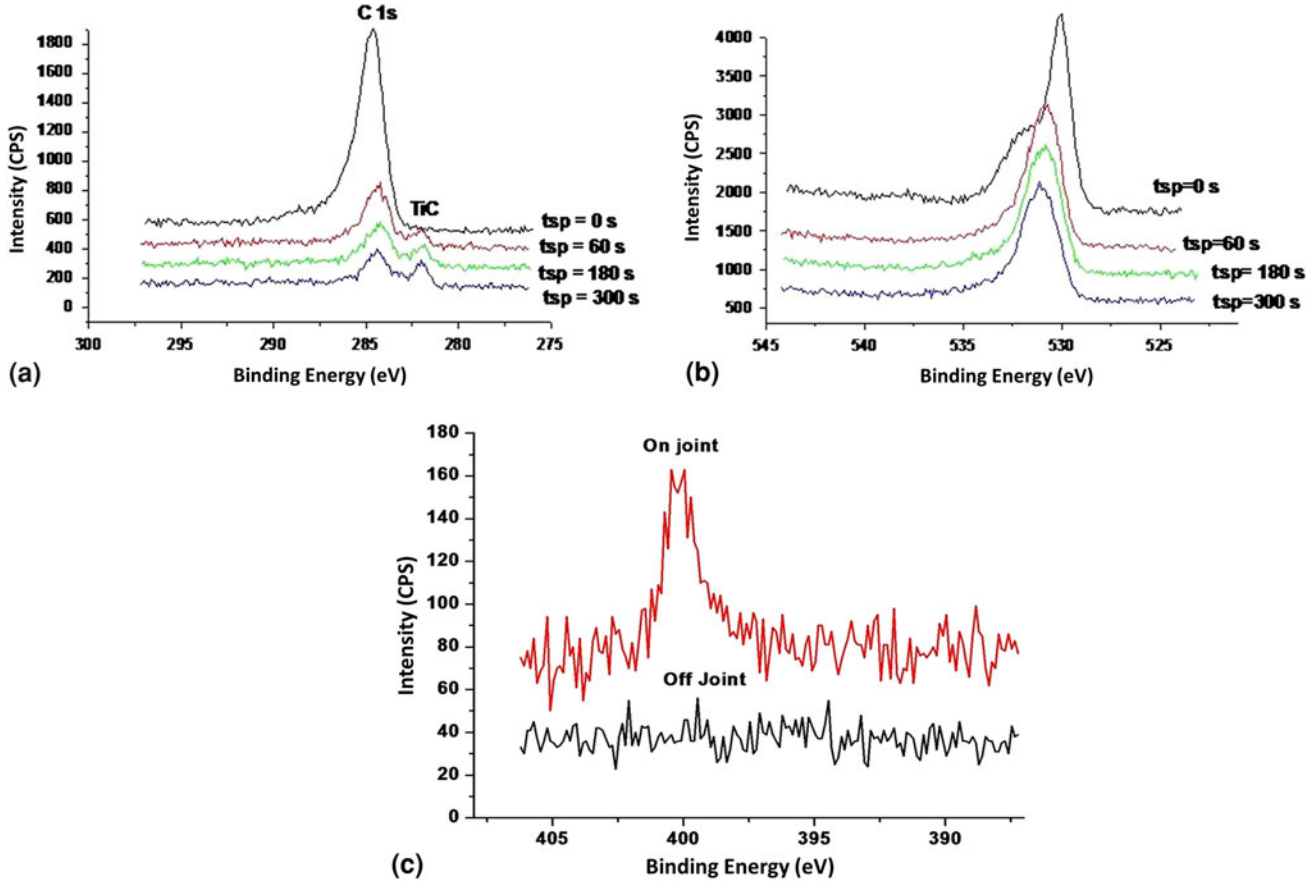

Fig. 7 (a) XPS C 1s spectra as a function of time for 200 nm thick Ti coated glass/PI system on Ti side (XPS spot dia. = 2 mm); (b) XPS O 1s spectra as a function of time for 200 nm thick Ti coated glass/PI system on Ti side (XPS spot dia. = 2 mm); (c) XPS N 1s spectra for 200 nm thick Ti coated glass/PI system on Ti side (XPS spot dia. = 0.2 mm)

This new peak corresponds to the reported carbon line in TiC (Ref 18), and it is therefore justified to conclude that the interface contains certain amount of Ti-C bonds.

Due to the aggressive nature of Ti, the vapor-deposited Ti reacts indiscriminately with triazine, polyimide, polystyrene, polyethylene, and epoxy films to form Ti-O, Ti-C, and Ti-N bonds (Ref 16, 19-22) and with fluoropolymers to form Ti-C, Ti-O, and Ti-F bonds (Ref 23). It was reported that when TiC fine particle are introduced to any thermoplastic resin matrix, forms a truly significant chemical bond. No other super-hard material known is able to bond with the same tenacity (Ref 24). Inclusion of Ti-C fine particle in any thermoplastic composite will maintain or slightly improve tensile strength (Ref 24). Reactive metals like Ti are known to have low mobility in polymers and to form relatively sharp interfaces with them (Ref 25, 26).

The O 1s spectra taken from the titanium side of the laser joint are shown in Fig. 7(b). The peak around 530 eV can be assigned (Ref 27) to oxygen from the natural TiO_2 layer of the titanium. The broad shoulder extending from 531 to 534.5 eV consists of at least two other components in the O 1s spectrum. These peaks indicate two types of assignments of the oxygen (Ref 28). Oxygen and moisture from the laboratory environment is expected to contribute in the region of 532-533 eV. Therefore, given the fact that exposing the samples to air before the insertion in the XPS analysis chamber, cannot be avoided. The only hypothesis for the unknown part of the contribution in that broad shoulder is due to polyimide oxygen atoms. Sputtering for 60 s or more causes a slight shift in the location of the main component of the O 1s line.

The width of the joint line (0.2 mm) is less than the area (2 mm) that has been analyzed by the XPS instrument. All collected spectra contained a ~10% contribution from the actual bond area and ~90% contribution from the non-laser-treated surface of the sample. Reduced XPS data collection area (0.2 mm) shows some interesting phenomena. Reduced collection area able to detect N on the joint line for on-joint of Ti side for 200 nm sputtered film. N 1s spectra on the joint area of Ti side of the sample confirm the existence of PI on the Ti surface (Fig. 7c).

In case of 400 nm Ti coated glass/polyimide system the results of high resolution spectrum of C 1s and Ti 2p3 on failed titanium surface has been described earlier in another paper of our group which is under review (Ref 29). Like 200 nm titanium coated glass/polyimide system, the high resolution spectra of C 1s line also revealed the existence of carbon configurations characteristics of polyimide (e.g., carbonyl group, -C=O around 288.4 eV). For this thickness the peaks that were observed in the region of 452-454 eV for high resolution XPS spectra of Ti 2p3 on Ti side provide a considerable understanding of the formations of TiC and TiO bonds as well as represents presence of metallic titanium (Ref 18, 27, 28). The O 1s spectra (Fig. 8) on-joint line of titanium side have a major peak at 530 eV with a pronounced shoulder 531-534 eV. This could be attributed to Oxygen from the

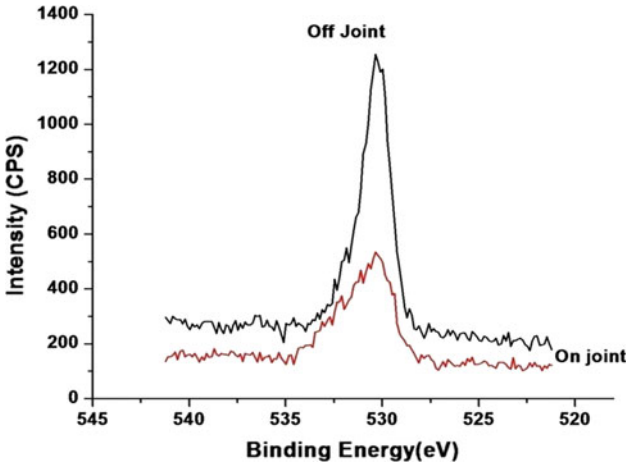

Fig. 8 XPS O 1s spectra for 400 nm thick Ti coated glass/PI system on Ti side (XPS spot dia. = 2 mm)

polyimide polymer which transferred onto the titanium side of the sample.

4. Conclusions

We present a detailed analysis of the interface of three different thicknesses of titanium coated glass and PI interface. The results show that the RMS roughness of titanium films increase with the increase in film thickness. Due to sufficiently higher roughness thicker film helps to improve mechanical interlocking property as well as bond strength. The results showed that film thicknesses in the range of 200-400 nm produced bond strength of about 29 MPa which is higher compared to thinner film of 50 nm thickness. The experimental results indicated that for 50 nm thick film volume of adhesion layer is not enough (Fig. 5a) to form good bonding and during laser joining process flashes were observed, which means high heat is produced in the joint area and heat transfer is not good in the area. From SEM/EDS analysis it has been found that the locus of failure shifted from the interface of metal and polymer for less rougher film (50 nm film thickness) to mixed mode failure which includes cohesive failure of polymer, failure in the interface of titanium/glass and glass itself for thicker and rougher film (200 and 400 nm thick film).

Finally, the XPS results showed formation of Ti-C, Ti-O, and >C=O bond on the interface for 200 and 400 nm titanium coated glass/imidex system. This bonding mechanism was supported by the O 1s peak at about 531 eV. Ti-C bond formation was supported by both C 1s and Ti 2p3 data. Besides the presence of N was observed on the titanium surface for thicker films (200 and 400 nm) which is also from polyimide. But 50 nm film failed to produce any chemical bond on the interface. It also can be concluded that to form good bonding between titanium and polymeric film, required titanium film thickness should be higher than 50 nm.

Acknowledgment

This work was supported by Michigan Economic Development Corporation (MEDC); Dr. Elias Shakour was the program monitor.

References

1. G. Dlubek, R. Buchhold, Ch. Hubner, and A. Nakladal, Water in Local Free Volumes of Polyimides: A Positron Lifetime Study, *Macromolecules*, 1999, **32**, p 2348–2355
2. K.K. Lee, J.P. He, A. Singh, S. Massia, G. Ehteshami, B. Kim, and G. Raupp, Polyimide-Based Intracortical Neural Implant with Improved Structural Stiffness, *J. Micromech. Microeng.*, 2004, **14**, p 32–37
3. K.D. Wise, D.J. Anderson, J.F. Hetke, D.R. Kipke, and K. Najafi, Wireless Implantable Microsystems: High-Density Electronic Interfaces to the Nervous System, *Proc. IEEE*, 2004, **92**, p 76–97
4. S. Metz, R. Holzer, and P. Renaud, Polyimide-Based Microfluidic Devices, *Lab Chip*, 2001, **1**, p 29–34
5. G. Newaz, A. Mian, T. Sultana, T. Mahmood, D.G. Georgiev, G. Auner, R. Witte, and H. Herfurth, A Comparison Between Glass/Polyimide and Titanium/Polyimide Microjoint Performances in Cerebrospinal Fluid, *J. Biomed. Mater. Res. A*, 2006, **79A**, p 159–165
6. A. Mian, G. Newaz, L. Vendra, N. Rahman, D.G. Georgiev, G. Auner, R. Witte, and H. Herfurth, Laser Bonded Microjoints Between Titanium and Polyimide for Applications in Medical Implants, *J. Mater. Sci. Mater. Med.*, 2005, **16**, p 229–237
7. S. Tamai, A. Yamaguchi, and M. Ohta, Melt Processible polyimides and Their Chemical Structures, *Polymer*, 1996, **37**, p 3683–3692
8. T. Kuroki, A. Shibuya, M. Torida, and S. Tamai, Melt-Processable Thermosetting Polyimide: Synthesis, Characterization, Fusibility, and Property, *J. Polym. Sci.: Part A*, 2004, **42**, p 2395–2404
9. M.J. Wild, A. Gillner, and R. Poprawe, Locally Selective Bonding of Silicon and Glass with Laser, *Sens. Actuators A*, 2001, **93**, p 63–69
10. G. Newaz, A. Mian, L. Vendra, D. Georgiev, T. Mahmood, G. Auner, R. Witte, and H. Herfurth, Mechanical Characterization of Laser Microjoints for Bioencapsulation, *Proceedings of the International Congress on Materials Science and Nanotechnologies, European Academy of Science, Brussels, Belgium,* Oct 2003
11. I. Bauer, UA Russek, H. Herfurth, R. Witte, S. Heinemann, G. Newaz, A. Mian, D.G. Georgiev, and G. Auner, Laser micro-joining of dissimilar and biocompatible materials, *Proceedings of SPIE-Photonics West Lase 2004: Lasers and Applications in Science and Engineering Conference, San Jose, California*, Jan 2004
12. F. Sari, W.-M. Hoffmann, E. Haberstroh, and R. Poprawe, Applications of laser transmission processes for the joining of plastics, silicon and glass micro parts, *Microsyst. Technol.*, 2008, **14**, p 1879–1886
13. M. Lu, Z. Qian, W. Ren, S. Liu, and D. Shangguan, Investigation of Electronic Packaging Materials by Using a 6-Axis Mini Thermo-Mechanical Tester, *Int. J. Solids Struct.*, 1999, **36**, p 65–78
14. N.J. Lubna, Laser bonding characteristics of sputtered titanium on glass with polymeric films, In *Material Science and Engineering*, Wayne State University, Detroit, p 1–189, 2009
15. A.J. Griffin Jr, and F.R. Brotzen, Effect of Thickness on the Transverse Thermal Conductivity of Thin Dielectric Films, *J. Appl. Phys.*, 1994, **75**, p 3761–3764
16. F.S. Ohuchi and S.C. Freilich, Metal Polyimide Interface—A Titanium Reaction-Mechanism, *J. Vac. Sci. Technol. A*, 1986, **4**, p 1039–1045
17. C. Girardeaux, G. Chambaud, and M. Delamar, The Polyimide (PMDA-ODA) Titanium Interface. 3. A Theoretical Study, *J. Electron Spectrosc.*, 1996, **77**, p 209–220
18. H. Ihara, Y. Kumashiro, A. Itoh, and K. Maeda, Some Aspects of ESCA Spectra of Single Crystals and Thin Films of Titanium Carbide, *Jpn. J. Appl. Phys.*, 1973, **12**, p 1462–1463
19. K. Konstadinidis, A.J. Taylor, A.C. Miller, and R.L. Opila, X-ray Photoelectron Study of Chemical Interactions at Ti/Polymer Interfaces, *J. Adhes.*, 1994, **46**, p 197–213
20. T. Tachibana, B.E. Williams, and J.T. Glass, Correlation of the Electrical Properties of Metal Contacts on Diamond Films with the Chemical Nature of the Metal-Diamond Interface. II. Titanium Contacts: A Carbide-Forming Metal, *Phys. ReV. B*, 1992, **45**, p 11975–11981
21. P. Bodo and J.E. Sundgren, Adhesion of Evaporated Titanium to Polyethylene: Effects of Ion Bombardment, Pretreatment, *J. Vac. Sci. Technol. A*, 1984, **2**, p 1498–1502
22. P. Bodo and J.E. Sundgren, Adhesion of Evaporated Titanium Films to Ion-Bombarded Polyethylene, *J. Appl. Phys.*, 1986, **60**, p 1161–1168
23. M. Du, R.L. Opila, and C. Case, Interface Formation Between Metals Cu, Ti and Low Dielectric Constant Organic Polymer FLARE™ 1.0, *J. Vac. Sci. Technol. A*, 1998, **16**, p 155–162

24. W.E.F. Thurber Jr., Creative Distinctive Grades of Abrasion-Resistant Plastics, *The Functional Fillers 95 Conference, Houston, Texas,* 1995
25. F. Faupel, R. Willecke, A. Thran, M. Keine, C. VonBechotolsheim, and T. Strunskus, Metal Diffusion in Polymers, *Defect and Diffusion Forum*, 1997, **143**, p 887–902
26. N. Main and Y. Serruys, Metallic Impurities Diffusion in a Polymer Film (Kapton) Under and Out of Irradiation, *Nucl. Instrum. Methods Phys. Res. B*, 1997, **131**, p 109–120
27. A. Turkovic' and D. Sokcevic, X-Ray Photoelectron-Spectroscopy of Thermally Treated TiO_2 Thin-Films, *Appl. Surf. Sci.*, 1993, **68**, p 477–479
28. H.F. Franzen, M.X. Umaña, J.R. McCreary, and R.J. Thorn, XPS Spectra of Some Transition Metal and Alkaline Earth Monochalcogenides, *J. Solid State Chem.*, 1976, **18**, p 363–368
29. N. Lubna, and G. Newaz, Analysis of Titanium Coated Glass and Imidex (PI) Laser Bonded Samples, *J. Mater. Eng. & Perform.,* 2011. doi:10.1007/s 11665-011-9900-9